Corrections for Response Errors in a Three-Component Propeller Anemometer[1]

THOMAS W. HORST

Atmospheric Physics Section, Battelle Memorial Institute, Pacific Northwest Laboratories, Richland, Wash. 99352

(Manuscript received 19 May 1972, in revised form 25 February 1973)

ABSTRACT

Methods of eliminating or reducing three types of errors found in the Gill *UVW* anemometer have been investigated by utilizing field experiments comparing this sensor with a three-component sonic anemometer. The non-cosine response of each of the three orthogonal propellers to a wind which is not parallel to the propeller axis was adequately corrected during computer processing of the data, using the manufacturer's wind-tunnel-measured calibrations. The accepted theory describing a propeller as a first-order system with a time constant $\tau = L/\bar{u}$ (where L is a distance constant characterizing the propeller inertia and $\bar{u}$ is the mean wind) was found to be only a fair description of the frequency response, probably due to dependence of L on properties of the flow, but was used to qualitatively delineate proper applications for this sensor. The threshold response was improved for the U and V components by orienting the anemometer so that the mean wind direction bisects the angle between the horizontal axis propellers. Improvement was also achieved for the vertical component of the wind by rotating the formerly vertical W propeller 45° into the horizontal, in the plane bisecting the horizontal propeller axes. The orthogonal components of the wind must then be calculated during computer processing of the data. Since for many applications the finite, but small, response threshold of the vertical component was not found to be a serious problem, the additional complication of this modification may be unnecessary.

1. Introduction

Proper use of a sensor requires knowledge of its response to the variable being measured. This knowledge can be employed to decide on the appropriateness of the sensor for a given application, to correct the data for improper response, or to serve as a guide for modification of the sensor to eliminate poor response characteristics. This approach has been taken with the Gill *UVW* anemometer, one of several anemometers considered by the Battelle-Pacific Northwest Laboratories Atmospheric Sciences Department for use in micrometeorological experiments.

The Gill *UVW* anemometer (Fig. 1) is a fixed array of three propeller anemometers, each of which has its axis of rotation oriented along one of three orthogonal directions, two in the horizontal (U and V) and one in the vertical (W). Each propeller drives a dc tachometer generator to provide an analog signal directly proportional to its rotation speed (Holmes *et al.*, 1964). Extensive response data derived from wind tunnel measurements are supplied by the manufacturer, but the final test of the anemometer must be made in a wind field which has a spectrum of eddies similar to that which will be measured. Tests in the atmosphere provide the proper input to the anemometer, but lack the well-defined flow of the laboratory experiment against which to compare the sensor output. This latter deficiency has been overcome by utilizing the three-component sonic anemometer (Model PAT 311) manufactured by Kaijo-Denki Co., Tokyo, whose response characteristics qualify it as an appropriate standard against which to compare the Gill anemometer.

Two sonic and two Gill anemometers (R. M. Young Co. Model 27002) were placed alternately about 1.5 m apart along a line normal to the expected mean wind direction with instrument centers at a height of 6.5 m (Fig. 1). Representative dimensions of these sensors are: *Gill* (height, 107 cm; arm length, 40 cm; propeller diameter, 23 cm), *sonic* (height, 48 cm; width, 45 cm; depth, 37 cm; acoustic path, 20 cm). Upwind of the measurement site was a fairly homogeneous fetch of sagebrush plants roughly 1 m high and spaced 1–3 m apart. Data from these four instruments were recorded on an analog tape recorder and later digitized at a rate of 100 points sec^{-1}. Statistics were computed for the Gill and sonic anemometer signals after averaging over successive 20-point blocks to produce data more consistent with the frequency response of the individual Gill propeller. These statistics have been utilized to compare the response of the Gill to that predicted from wind tunnel measurements, and to test methods for eliminating or reducing errors due to shortcomings in three types of response: cosine response, frequency response, and threshold response. These are discussed

[1] This paper is based on work performed under U. S. Air Force Contract F33615-M-5009 and U. S. Atomic Energy Contract AT(45-1)-1830.

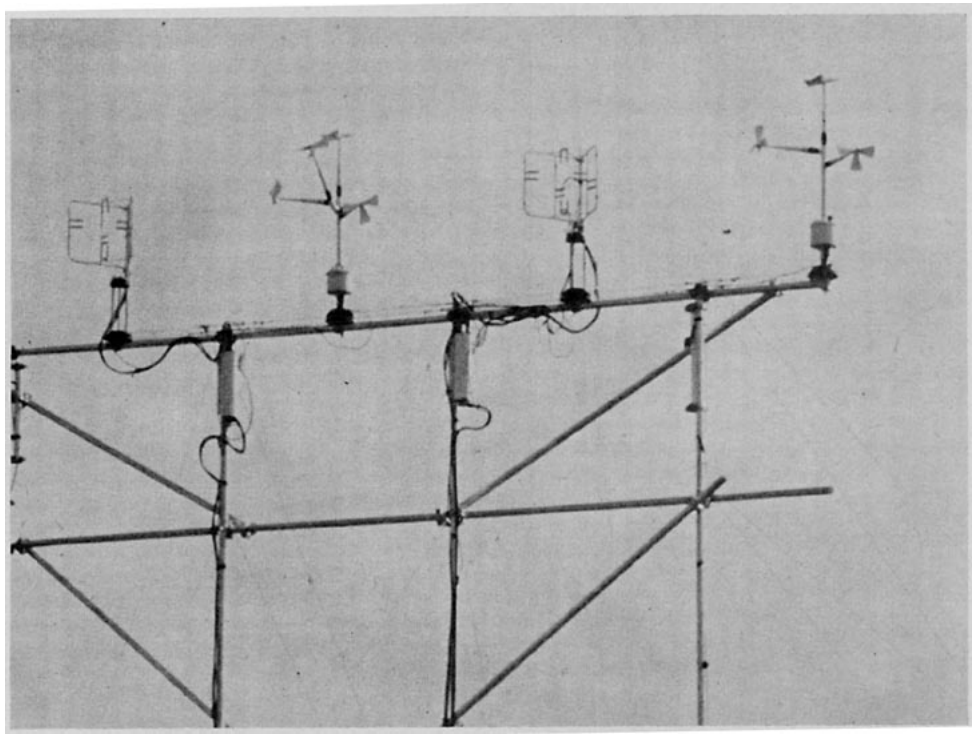

FIG. 1. Field array for comparing sonic and Gill anemometers. Instruments are from left to right: sonic 153; modified *UVR* Gill; sonic 150; *UVW* Gill. See Section 4 for a description of the modified Gill anemometer.

individually below and conclusions are then drawn on the proper use of the Gill anemometer.

2. Cosine response

The Gill propeller was designed to follow a cosine response, sensing only that component of the wind parallel to the propeller shaft. However, the manufacturer's calibration shows a deviation from the cosine curve which becomes worse as the angle between the wind and the propeller axis increases from 0° to 90° (Horizontal axis, Table 1). The cosine response will be worst for the *W* arm, the wind fluctuating about an angle of 90°, and hence this arm is calibrated for a 25% greater output than the horizontal arms to bring the response closer to the cosine law within the expected input range of 60°–120° (Vertical axis, Table 1).

TABLE 1. Fraction of cosine response for Gill anemometer.*

Horizontal axis				Vertical axis	
Angle (deg)	Fraction	Angle (deg)	Fraction	Angle (deg)	Fraction
5	1.00	95	0.75	60	1.00
10	0.99	100	0.86	65	0.97
15	0.99	105	0.86	70	0.93
20	0.98	110	0.85	75	0.89
25	0.97	115	0.82	80	0.86
30	0.95	120	0.81	85	0.75
35	0.93	125	0.82	90	—
40	0.90	130	0.84	95	0.75
45	0.87	135	0.88	100	0.92
50	0.84	140	0.92	105	0.96
55	0.81	145	0.94	110	0.96
60	0.78	150	0.96	115	0.97
65	0.76	155	0.97	120	0.96
70	0.70	160	0.98		
75	0.69	165	0.99		
80	0.66	170	0.99		
85	0.57	175	0.99		

* Calculated from calibration curve supplied by R. M. Young Co. [see Drinkow (1972, Fig. 3) for reproduction].

Some immediate conclusions can be drawn from this information. If both components of the horizontal wind vector are of equal interest, the smallest total percent error due to non-cosine response (13% for each component) will be obtained by orienting the anemometer so that the mean wind vector makes an angle of 45° to both the *U* and *V* arms. Certain other measurements, such as the total wind speed, will contain the least cosine response error if one of the propeller axes is lined up with the direction of the mean wind, but the finite threshold response of the propellers makes this an undesirable orientation (see Section 4). Due both to this latter consideration and to the fact that most detailed micrometeorological studies require knowledge of the vector wind, the former orientation is used operationally at Battelle-Pacific Northwest Laboratories and was used during the comparison experiments with the sonic anemometer.

Power spectra obtained by the fast-Fourier transformation of 8192 data points (~28 min of data) from

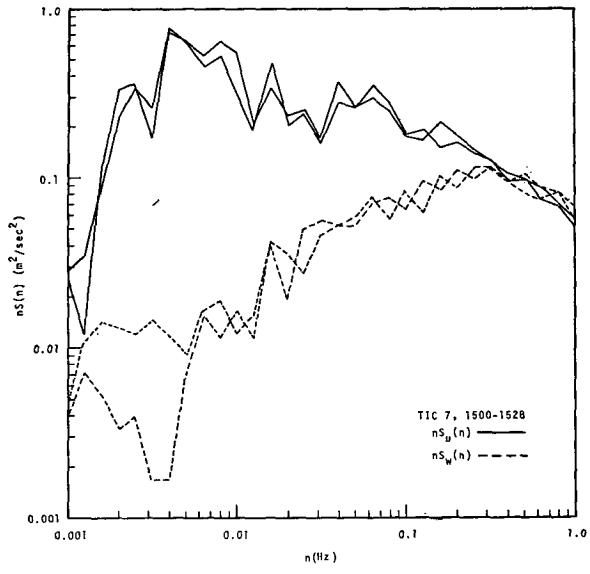

FIG. 2. Power spectra of the longitudinal and vertical wind components as measured by adjacent sonic anemometers.

one of the comparison tests are shown in Figs. 2–4. Fig. 2 shows the longitudinal and vertical power spectra of the two sonic anemometers. Since differences between these two spectra can be attributed mainly to differences in the winds being sampled, this figure gives a measure of the agreement to be expected between the sonic and Gill anemometers when all errors are corrected for in the propeller anemometer. The difference in the vertical spectra at $1.5\text{–}5\times10^{-3}$ Hz might be due to interference between the instruments, but probably reflects actual inhomogeneity in the wind field since the mean wind vector was only 14° from being normal to the line of instruments. Figs. 3 and 4 compare the Gill spectra (dotted lines) to the sonic spectra (solid lines) for both the longitudinal and vertical wind components. Below 0.3 Hz, the differences are principally due to the non-cosine response, and the manufacturer's calibration (Table 1) has been used to correct each data point in the time series for this error. The spectra of the corrected data, plotted as dashed lines in Figs. 3 and 4, agree well with those measured by the sonic.

The cosine correction is performed by a computer subroutine during preliminary data handling (Horst, 1972). Since the correction for each measured wind component is a function of the angle between that propeller axis and the wind vector (or, equivalently, the cosine of the angle) and since the correct wind vector may have an orientation different from that of the uncorrected wind vector, an iterative scheme must be used until the results converge. The direction cosines are calculated from the three wind components, the appropriate corrections are applied to the data, and new direction cosines are calculated from the corrected wind components. Less than six repetitions of these steps is normally adequate for successive direction cosine sets to agree within ±0.02. Figs. 2–4 display the agreement achieved by thus correcting the propeller anemometer. These figures can be summarized by integrating the spectra to obtain the variance below 0.3 Hz. (Above this frequency there are additional errors, discussed in Section 3, peculiar to the higher frequencies.) The sonic anemometers agree within about 6% of each other for all components while the adjacent sonic and Gill anemometers chosen for Figs. 3 and 4 agree within 3% for the variance of the longitudinal component and within 8% for the vertical component.

Table 2 lists various statistics from all four anemometers for the data string utilized above and also for the following 28-min period to provide a larger sampling on which to judge the effectiveness of the cosine correction. The Gill data have here been corrected for cosine response and the second moments $(\sigma_u,\sigma_v,\sigma_w,u_*)$ have been low-pass filtered at 0.3 Hz as mentioned above. With the exception of σ_v, the statistics from the Gills are consistent with the approximately 5% scatter indicated by the sonic anemometers. The data for σ_v stand out because the Gills are consistently higher than the sonics (averaging about 5%), although the individual instruments compare no worse for this statistic than for the others shown. This fact has not been satisfactorily explained, nor is it known whether it is significant.

Since the cosine correction is a function of the direction of the wind vector relative to the anemometer, it is determined and applied for each data point. The variability in wind direction found in the atmosphere for a typical "steady state" period of 20–60 min is too large to correct statistics calculated from the raw data simply

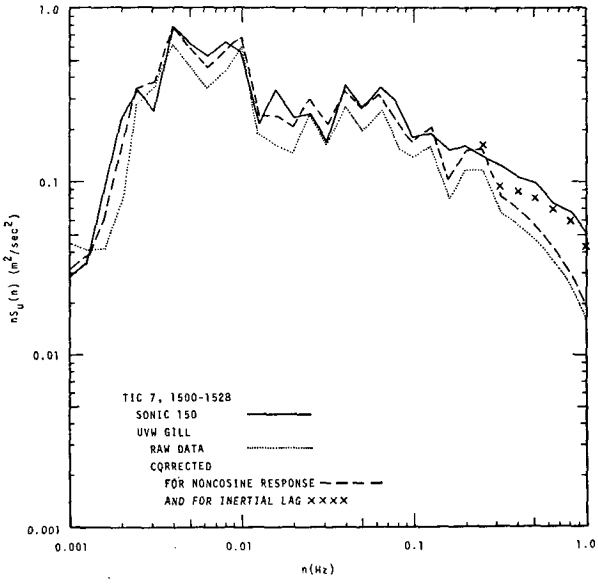

FIG. 3. Power spectra of the longitudinal wind component as measured by adjacent sonic and Gill *UVW* anemometers.

on the basis of the mean wind direction. However, the proper cosine correction for certain of these raw statistics can be calculated from a simple model of the fluctuating wind vector, which assumes that the vector components in spherical coordinates (wind speed, azimuth angle and elevation angle) are independent random variables, and that the azimuth and elevation angles have Gaussian distributions. This model requires estimates of the mean wind vector and of the variances of the spherical components of the wind to predict corrections to these same statistics, and hence an iterative process is required if only the raw Gill data are available.

Tests of this model using Gill anemometer data show that it works very well for predicting corrections to the mean wind vector and to the variance of the vertical wind component, and almost as well for the variances of the horizontal wind components. Apparently, the correlations among the spherical wind components are negligible for the former statistics, but not quite for the latter. Obviously these correlations could not be expected to be negligible for quantities such as the Reynolds stress, which would be identically zero under that assumption. Details of the model and its performance are given in the Appendix. Its utility is limited in its present form and in many cases, therefore, it is still necessary to correct each data point for noncosine response.

3. Frequency response

The dynamic response of a propeller to a change in the wind is described, neglecting bearing friction, by a first-order differential equation,

$$\tau dU/dt = u_P - U, \tag{1}$$

where U is the indicated wind speed, u_P the component of the wind sensed by the propeller, and τ a time constant characteristic of the system. It has been shown (MacCready and Jex, 1964) that for a propeller with its axis parallel to the direction of the mean wind

$$\tau = L/\bar{u}, \tag{2}$$

where $\bar{u}$ is the mean wind speed and L a distance constant independent of the mean wind. The measurements of Camp *et al.* (1970) imply that this relationship is also valid for flow which is not parallel to the propeller axis (see also Clink, 1971). Camp's results appear to be contradicted, however, by the reported measurements of Gill (McBean, 1972) which show that L increases with the angle between the propeller axis and the direction of flow. Fichtl and Kumar (unpublished manuscript) have analyzed a large quantity of atmospheric data from a vertically oriented Gill propeller and conclude that L is also a function of the turbulence level.

For a first-order system, as defined by Eq. (1), the response of the propeller to a sinusoidal input,

$$u_P = \mu \sin\omega t, \tag{3}$$

would be

$$U = \mu(1+\omega^2\tau^2)^{-\frac{1}{2}} \sin(\omega t - \beta), \tag{4}$$

where β is a phase lag,

$$\beta = \tan^{-1}\omega\tau. \tag{5}$$

Thus, the power spectra for the Gill anemometer are attenuated by a frequency-dependent factor $(1+4\pi^2 n^2 L^2/\bar{u}^2)^{-1}$. This will give a half-power point, corresponding to a reduction in the power spectrum of 50%, at a frequency

$$n_{\frac{1}{2}} = \bar{u}/2\pi L. \tag{6}$$

L is listed by the manufacturer as 0.95 m, giving a time

TABLE 2. Wind statistics from two 28-min segments of instrument comparison experiment TIC 7.

	$\bar{u}$ (m sec^{-1})	$\bar{\theta}$ (deg)	σ_u (m sec^{-1})	σ_v (m sec^{-1})	σ_w (m sec^{-1})	u_* (m sec^{-2})
1500–1528						
Sonic 153	5.34	7	1.26	1.30	0.47	0.42
Gill 4C	5.52	7	1.28	1.38	0.46	0.45
Sonic 150	4.91	7	1.30	1.26	0.48	0.45
Gill 3C	4.98	6	1.28	1.33	0.50	0.49
1528–1556						
Sonic 153	5.72	20	1.19	1.01	0.44	0.44
Gill 4C	6.12	20	1.24	1.05	0.45	0.43
Sonic 150	5.41	20	1.18	0.98	0.47	0.42
Gill 3C	5.65	20	1.15	1.02	0.51	0.44

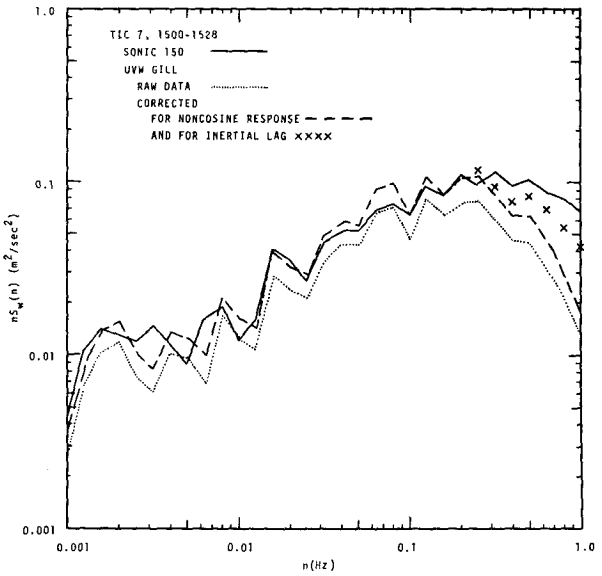

FIG. 4. Power spectra of the vertical wind component as measured by adjacent sonic and Gill *UVW* anemometers.

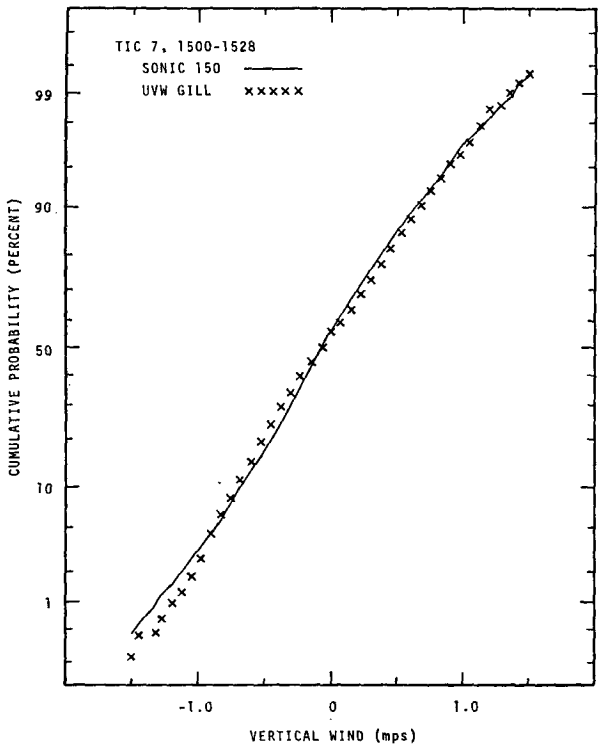

FIG. 5. Probability distributions of the vertical wind component as measured by adjacent sonic and Gill *UVW* anemometers.

constant of 0.183 sec and a half-power point of 0.87 Hz for the mean wind of 5.2 m sec^{-1} observed for the period analyzed for Figs. 2–4.

Actually the Gill anemometer also incorporates an RC low-pass filter to remove an approximately 10% ripple from the dc generator signal. The response of the filter is also described by a first-order differential equation, characterized by a time constant

$$\tau_f = \mathrm{RC} = 0.03 \text{ sec}, \tag{7}$$

where R is the resistance and C the capacitance of the parallel circuit. This corresponds to a half-power point of 5.3 Hz. The combined effect of the propeller response and the RC filter is multiplicative in the amplitude attenuation and additive in the phase angle, i.e.,

$$U = \mu[(1+\omega^2\tau^2)(1+\omega^2\tau_f^2)]^{-\frac{1}{2}} \sin(\omega t - \beta - \beta_f). \tag{8}$$

However, the RC filter produces only a 1% reduction in the signal at the frequency corresponding to the half-power point of the propeller response. It will therefore not be considered in the following discussion.

The spectra from the Gill anemometer in Figs. 3 and 4 which have been corrected for the non-cosine response are seen to rapidly drop below the spectra from the sonic anemometer for frequencies $\gtrsim$0.25 Hz. These spectra have been additionally corrected for the inertial lag of the propeller and plotted as crosses in Figs. 3 and 4, using the calculated time constant of 0.183 sec. This produces a fair correction of the spectra, but a better correspondence with the sonic data could be achieved by using time constants of 0.23 and 0.26 sec for the horizontal and vertical axes, respectively, This would imply distance constants of 1.20 and 1.35 m.

The larger distance constants may be due to the mean flow not being parallel to the propeller axis, since the wind direction was at an angle of roughly 45° to each of the horizontal axes and 90° to the vertical axis. This would agree qualitatively with the wind tunnel measurements of Gill. If, in fact, the distance constant is a strong function of the angle between the wind direction and the propeller axis, the U and V axes will, in general, have different time constants characterizing their response and the wind components along a rotated set of coordinates, such as that defined by the direction of the mean wind, will no longer have a simple response as described by Eq. (1). The frequency response of a propeller in a nonaxial, highly turbulent flow is still poorly understood, however, and additional investigation needs to be carried out in this area before frequency response corrections can be quantitatively reliable.

The need for frequency response corrections can be avoided by using the Gill anemometer only in situations in which the response error is less than an acceptable limit. This is possible because the size of the eddies which contribute to turbulence statistics change as a function of height and thermal stability. Eq. (4) and spectral models of various statistics are used in Section 5 to present useful results of this type.

4. Threshold response

As seen in Table 1, the non-cosine response error of the Gill becomes most critical as the angle between the wind and the propeller axis approaches 90°. As the component of the wind available to rotate the propeller (i.e., that parallel to the propeller axis) becomes smaller, the torque on the propeller eventually becomes less than the amount necessary to overcome the internal friction of the rotating parts. Increasing slippage from the calibrated rotation rate of 3.15 revolutions per meter of wind passage occurs as the wind drops below a speed of 1 m sec^{-1} until, at the threshold level of 20 cm sec^{-1}, the wind is unable to turn the propeller.

Since the mean wind is at an angle of 90° to the W arm of the Gill anemometer, the threshold response problem is most evident in this component. The vertical axis propeller must frequently pass through the threshold "dead" region as the vertical component of the wind approaches zero or changes sign. Fig. 5 is a plot of the cumulative probability distribution of the vertical component as measured by the sonic and Gill anemometers. A number of vertical gusts sensed by the sonic anemometer have, to some degree, not been recorded properly by the propeller. (It should be noted that the Gill data have been corrected for cosine response as described in Section 2. If they had not, the

cumulative probability distribution for the Gill anemometer would have been a line of greater slope than that for the sonic, the two lines crossing at 50% probability and zero wind speed.) A peculiar property of the dc generator transducer is the production of small spikes in the output, caused by the sudden stopping and starting of propeller rotation as the wind passes into and out of the dead region. This phenomenon has been observed on strip chart recordings of the data and is evident in the probability distribution shown in Fig. 5.

If the U arm of the anemometer is directed into the wind, the threshold response problem is also serious for the V arm. When both the longitudinal and lateral components of the turbulence are of interest, as is true in most cases, the anemometer must therefore be oriented so that the mean wind is between the U and V propeller axes. A similar method can be used to avoid the threshold problem for the W arm, by tilting it 45° into the mean wind. This can be accomplished either by tilting the entire UVW anemometer or by replacing the existing W arm with a nonorthogonal arm in the vertical plane. The three propellers of either configuration are all facing into the mean wind and will always rotate in the same direction.

Such a nonorthogonal (UVR) array was constructed and tested in the comparison experiment. A normal UVW Gill was modified by the addition of a fourth propeller in the vertical plane bisecting the U and V axes and at an angle of 45° to the vertical (Fig. 1). The normal W arm was left in place for comparison between the data from the UVW and UVR arrays, although the UVW data presented here are from the unmodified Gill anemometer. The vertical wind component is determined from the UVR array by removing the contributions of the horizontal wind from the wind measured by the R arm. Proper resolution of the orthogonal components of the wind requires that the data be first corrected for non-cosine response, an optional procedure for the normal UVW array.

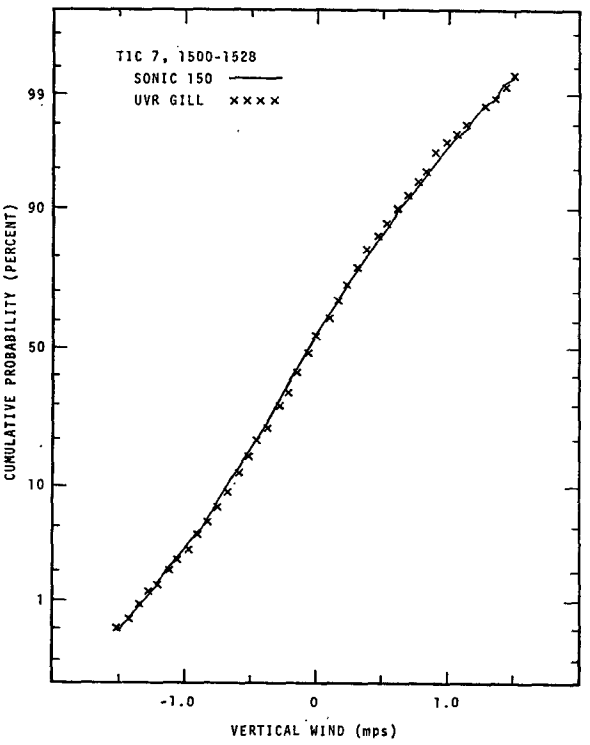

FIG. 6. Probability distributions of the vertical wind component as measured by adjacent sonic and Gill UVR anemometers.

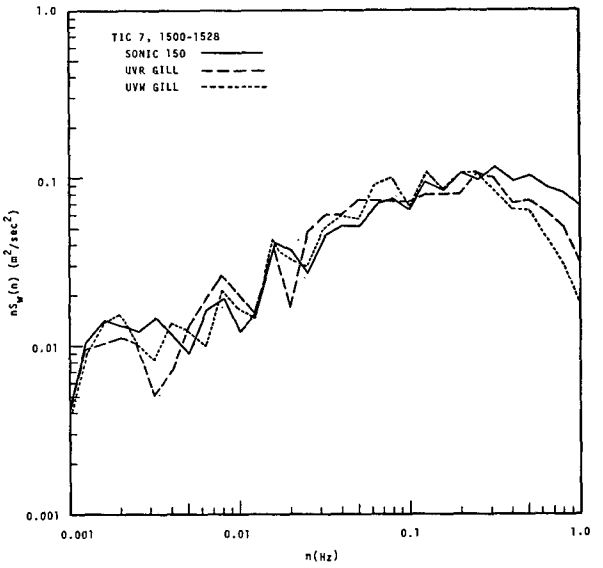

FIG. 7. Power spectra of the vertical wind component as measured by adjacent sonic, Gill UVR and Gill UVW anemometers.

Fig. 6 shows the cumulative probability distributions of the vertical wind as measured by the UVR anemometer and the same sonic anemometer used in Fig. 5. The improvement is quite obvious, the most noticeable remaining differences occurring for the stronger vertical gusts (which would again be close to normal to the axis of the tilted arm). The change is not nearly so meritorious, however, when other statistics are compared. The only consistent difference in the vertical power spectra (Fig. 7) is found in the highest frequencies and is most likely due to the decrease in the distance constant associated with a change of the angle between the mean flow and the propeller axis from 90° to 45° (see Section 3). One drawback of the UVR array is demonstrated by a small positive portion in the high frequencies of the uw cospectrum derived from this anemometer. It has apparently been erroneously produced by inadequate resolution of the horizontal and vertical fluctuations measured by the R arm. Apparently, then, the threshold response in the W axis has properties, including symmetry, which reduce the resulting error in many normally utilized statistics, such as $nS_w(n)$, σ_w, $u_*^2=\overline{uw}$, etc., to a tolerable level, and the improve-

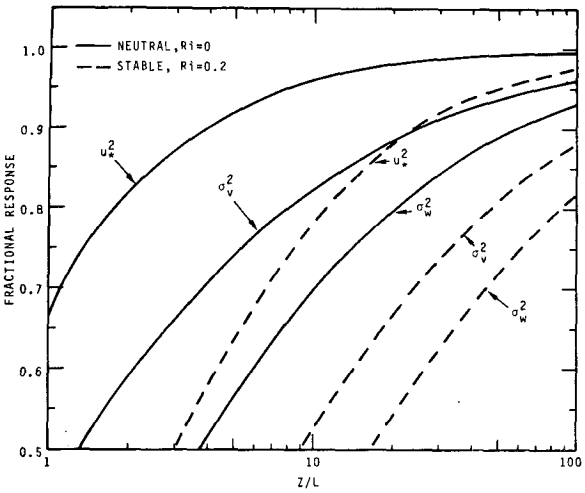

FIG. 8. Fractional response of an anemometer, characterized by a distance constant L, to various statistics as a function of height and stability.

ment afforded by a tilted "W" axis may be of value for the measurement of only a limited number of statistics.

5. Discussion

Analysis of the data from the comparison experiment between the sonic and Gill UVW anemometers has shown that the most effective correction that can be applied to data from the Gill anemometer is that for non-cosine response. This adequately compensates for the major source of error below about 0.3 Hz. Tests with an altered propeller array designed to eliminate the threshold error of the vertical axis propeller demonstrated that this aspect of the response does not seriously affect the commonly computed statistics. Threshold response is easily eliminated for the horizontal components by orienting the anemometer with the mean wind direction bisecting the angle between the U and V arms. This configuration is also recommended for minimizing the total cosine response error of the horizontal axis propellers.

The Gill data can be corrected for frequency response, to a fair approximation, by treating the anemometer as a first-order system with a time constant $\tau=L/\bar{u}$. Unfortunately, the distance constant L is not a function solely of the propeller design. It also depends on the properties of the flow, most noticeably the angle between the mean wind and the propeller axis, to a degree that is not insignificant for quantitative response correction. Additional research is needed to better define this functional dependence.

The dependence of L on the flow properties need not be considered, however, in deriving guidelines for proper utilization of the anemometer. Knowledge of the spectral distributions of the desired flow statistics can be combined with the response characteristics of the anemometer to delineate the circumstances in which the aneommeter will perform to the desired accuracy. Uncertainties in the spectral distributions obviate refinements in the distance constant. Examples are given below for the measurement of the variances of the three components of the wind and for the measurement of the Reynolds stress.

Kaimal *et al.* (1972) have modeled the spectral distributions of these statistics for an adiabatic or neutrally stable atmosphere as a function of the natural frequency, $f=nz/\bar{u}$:

$$nS_u(n)/u_*^2=105f/(1+33f)^{5/3}, \quad (9)$$

$$nS_v(n)/u_*^2=17f/(1+9.4f)^{5/3}, \quad (10)$$

$$nS_w(n)/u_*^2=2f/[1+5.3(f)^{5/3}], \quad (11)$$

$$-nC_{uw}(n)/u_*^2=14f/(1+9.6f)^{2.4}. \quad (12)$$

Here S_u, S_v, S_w are the power spectra for the longitudinal, lateral and vertical wind components, and C_{uw} is the cospectra between the longitudinal and vertical wind components. The integrals of these quantities over all frequencies give the variances of the three components of the wind ($\sigma_u^2,\sigma_v^2,\sigma_w^2$) and the Reynolds stress u_*^2. Taking account of the inertial properties of the propeller according to Eq. (4), the measured statistic will be

$$\sigma_m^2=\int_0^\infty S(n)(1+n^2/n_1^2)^{-1}dn, \quad (13)$$

where $n_1=z/(2\pi L)$. These integrals have been evaluated numerically for Eqs. (9)–(12) and curves have been plotted in Fig. 8 showing the fraction of u_*^2, σ_v^2 and σ_w^2 measured by the anemometer in neutral conditions as a function z/L, the height normalized by the distance constant. The curve for σ_u^2 is slightly below that for u_*^2.

Since in a stable atmosphere the spectral distributions of these statistics are shifted to higher frequencies, the Gill anemometer will respond to a smaller fraction of the true quantity. The opposite situation occurs in an unstable atmosphere. Hence, the stable atmosphere represents the more serious situation. Kaimal (1972) has modeled the spectral distributions for the stable case as

$$nS_\alpha(n)/\sigma_\alpha^2=0.164(f/f_0)/[1+0.164(f/f_0)^{5/3}], \quad (14)$$

$$-nC_{uw}(n)/u_*^2=0.88(f/f_0)/[1+1.5(f/f_0)2.1], \quad (15)$$

where

$$(f_0)_u=0.5\ \mathrm{Ri}, \quad (16)$$

$$(f_0)_v=1.5\ \mathrm{Ri}, \quad (17)$$

$$(f_0)_w=2.8\ \mathrm{Ri}, \quad (18)$$

$$(f_0)_{uw}=3.1\ \mathrm{Ri}, \quad (19)$$

and Ri is the gradient Richardson number, a common quantifier of atmospheric stability. The Richardson number is negative for unstable conditions, zero for

neutral, and positive for stable. At Richardson numbers greater than the critical value of approximately 0.2, turbulent fluctuations are damped by the stable stratification of the atmosphere, the flow becomes laminar, and (14)–(19) are no longer valid. Hence, this limit represents the worst case for which we can estimate the fractional response. This has been done numerically, again using Eq. (13), and the results are also shown in Fig. 8. In this case also the curve for σ_u^2 is slightly below that for u_*^2.

Fig. 8 can be used in two different ways. Given a required accuracy for the measurement of one of these quantities, it will provide the lowest height at which the anemometer can be located. Alternatively, the graph estimates the error to be expected in the measurement of these statistics at a predetermined height. The neutral curves probably represent an optimistic estimate of the average response for all stabilities and the stable curves, as mentioned above, correspond to the worst case. Note that the vertical variance will be poorly measured in many micrometeorological situations and that the Gill anemometer performs poorly for all these statistics below 20 m in the extreme stable situation.

If operation of the Gill anemometer within an unsatisfactory portion of Fig. 8 cannot be avoided, spectral models such as presented in Eqs. (17), (22) and (23) can also be utilized to correct the desired statistic to some degree, but this should be done only with a clear realization of all of the limitations involved. The most simple example of this approach would be an extension of the $-5/3$ slope of the power spectra in the inertial subrange when the unattenuated response of the anemometer extends into the low frequency end of this region. In most cases this method would require spectral analysis of the data to be corrected.

Acknowledgments. Messrs. O. B. Abbey, J. C. Draper, A. G. Dunbar and D. C. Powell aided in collecting and processing the data from the instrument comparison experiment. Their cheerful help is gratefully appreciated.

APPENDIX

Corrections for Non-Cosine Response to be Applied to Raw Statistics

In order to correct statistics computed from the Gill data for non-cosine response, rather than correct each data point, a simple model is used to predict the corrections as a function of the mean wind direction and its horizontal and vertical variances. This model hypothesizes that the spherical components of the wind (S,θ,ϕ) are independent, random variables and that the azimuth and elevation angles have normal distributions. The mean of any function of these angles is then

$$\overline{f(\theta,\phi)}=(2\pi\sigma_\theta\sigma_\phi)^{-1}\int_{-\infty}^{\infty}\int f(\theta,\phi)\times\exp[-(\theta-\bar{\theta})^2/(2\sigma_\theta^2)-\phi^2/(2\sigma_\phi^2)]d\theta d\phi. \quad \text{(A1)}$$

For example, the mean wind along the U axis of the Gill anemometer is

$$\bar{U}=\bar{S}\,\overline{\cos\theta}\;\overline{\cos\phi}=\bar{S}\cos\bar{\theta}\exp(-\tfrac{1}{2}\sigma_\theta^2)\exp(-\tfrac{1}{2}\sigma_\phi^2), \quad \text{(A2)}$$

where the azimuth angle θ is measured from the U arm and the elevation angle ϕ is measured from the horizontal. The wind actually measured by this arm will be reduced by $F(\theta)$, the fractional non-cosine response (Table 1):

$$\bar{U}_m\approx\bar{S}\,\overline{F(\theta)\cos\theta}, \quad \text{(A3)}$$

where the fluctuations in elevation angle have been ignored with respect to the larger fluctuations in azimuth. The mean correction for non-cosine response along the U axis is then

$$\bar{U}/\bar{U}_m=\overline{\cos\theta}/\overline{F(\theta)\cos\theta}, \quad \text{(A4)}$$

and it can be easily shown that the appropriate correction to the mean wind speed is

$$\bar{u}/\bar{u}_m=[(\bar{U}_m/\bar{U})\cos^2\bar{\theta}+(\bar{V}_m/\bar{V})\sin^2\bar{\theta}]^{-1}, \quad \text{(A5)}$$

where

$$\bar{\theta}=\tan^{-1}(\bar{V}/\bar{U}). \quad \text{(A6)}$$

The mean correction can also be calculated for the vertical variance,

$$\overline{W^2}/\overline{W^2}_m=\overline{\sin^2\phi}/\overline{F^2(\phi)\sin^2\phi}. \quad \text{(A7)}$$

The horizontal variances are similarly treated, but with a few complications due to the fact that the horizontal wind components have a non-zero mean. In this case, we must begin with

$$\overline{U'^2}=\overline{U^2}-\bar{U}^2\approx\bar{S}^2\,\overline{\cos^2\theta}-\bar{S}^2\,\overline{\cos\theta}^2, \quad \text{(A8)}$$

where the vertical angle fluctuations have again been ignored. Note that the correction to the U variance, $\overline{U'^2}/\overline{U'^2}_m$, will also be a function of $\bar{S}^2/\bar{S}^2$. Of more interest is the variance of the wind component aligned with the mean wind,

$$\overline{u'^2}=\overline{U'^2}\cos^2\bar{\theta}+2\overline{U'V'}\sin\bar{\theta}\cos\bar{\theta}+\overline{V'^2}\sin^2\bar{\theta}, \quad \text{(A9)}$$

where, in addition to $\overline{U'^2}$ and $\overline{V'^2}$, we must now also calculate

$$\overline{U'V'}=\overline{UV}-\bar{U}\bar{V}\approx\overline{\bar{S}^2\sin\theta\cos\theta}-\bar{S}^2\,\overline{\sin\theta}\;\overline{\cos\theta}. \quad \text{(A10)}$$

The lateral variance $\overline{v'^2}$ is described by an equation

TABLE A1. Correction factors for non-cosine response to be applied to raw statistics.

$\bar{\theta}$ (deg)	Correction factors for $\bar{U}$ 5°	10°	σ_θ 15°	20°	25°	Correction factors for $\overline{W^2}$ σ_ϕ (deg)	Correction	σ_ϕ (deg)	Correction	σ_ϕ (deg)	Correction
0	1.00	1.01	1.01	1.02	1.03	1.0	4.45	4.0	1.65	7.0	1.33
5	1.01	1.01	1.01	1.02	1.03	1.2	3.78	4.2	1.62	7.2	1.32
10	1.01	1.01	1.02	1.02	1.03	1.4	3.38	4.4	1.58	7.4	1.31
15	1.01	1.02	1.02	1.03	1.04	1.6	3.03	4.6	1.55	7.6	1.30
20	1.02	1.03	1.03	1.04	1.04	1.8	2.75	4.8	1.52	7.8	1.29
25	1.03	1.04	1.04	1.05	1.05	2.0	2.52	5.0	1.50	8.0	1.28
30	1.05	1.06	1.06	1.06	1.06	2.2	2.35	5.2	1.47	8.2	1.27
35	1.08	1.08	1.08	1.08	1.08	2.4	2.21	5.4	1.45	8.4	1.26
40	1.11	1.10	1.10	1.10	1.09	2.6	2.10	5.6	1.43	8.6	1.25
45	1.14	1.13	1.13	1.11	1.10	2.8	2.00	5.8	1.42	8.8	1.25
50	1.18	1.17	1.15	1.14	1.12	3.0	1.92	6.0	1.40	9.0	1.24
55	1.22	1.21	1.18	1.16	1.14	3.2	1.85	6.2	1.38	9 2	1.23
60	1.27	1.24	1.21	1.18	1.15	3.4	1.79	6.4	1.37	9.4	1.23
65	1.31	1.28	1.24	1.21	1.17	3.6	1.74	6.6	1.35	9.6	1.22
70	1.35	1.32	1.28	1.23	1.19	3.8	1.70	6.8	1.34	9 8	1.12
75	1.39	1.36	1.31	1.26	1.21					10.0	1.21
80	1.46	1.14	1.36	1.30	1.25						
85	1.56	1.53	1.49	1.42	1.34						

similar to (A9), and the corrections are again calculated as $\overline{u'^2}/\overline{u'^2}_m$ and $\overline{v'^2}/\overline{v'^2}_m$.

Using the theory outlined above, correction factors have been calculated for the means and variances of the three components of the wind. The corrections to $\bar{U}$ and $\overline{W^2}$ have been listed in Table A1 as functions of $\bar{\theta}$, σ_θ, σ_ϕ. These predicted corrections have also been compared with the actual, point-by-point cosine corrections for three 20-min segments of Gill data in Table A2. The comparison is best for the mean wind statistics and worst for the horizontal variances, although the predicted correction is still fairly good in all cases. Two reasons may be given for the greater discrepancies in the horizontal variances. One is simply the fact that it is a second-order statistic. The other is found in Eq. (A10). The model we have assumed predicts that $\overline{u'v'}\equiv 0$, which is valid for a truly horizontally homogeneous flow but is not strictly the case for the data presented here. Apparently correlation between the spherical components of the wind should not be neglected for the calculation of $\overline{U'V'}$ and this contributes to the small but finite errors in predicting the corrections to the horizontal variances.

It was originally thought that the discrepancies found in the horizontal variance corrections were due to making the approximation noted for Eqs. (A3) and (A8), i.e.,

$$F[\cos^{-1}(\cos\theta\cos\phi)]\approx F(\theta), \qquad \text{(A11)}$$

TABLE A2. Comparison of point-by-point cosine response correction to correction of raw statistics predicted from simple wind model for three 20-min segments of experiment TIC 7.

	$\bar{U}$ (m sec^{-1})	$\bar{V}$ (m sec^{-1})	$\bar{u}$ (m sec^{-1})	$\bar{\theta}$ (deg)	σ_v^2 (m^2 sec^{-2})	σ_v/w (deg)	σ_w^2 (m^2 sec^{-2})	$\sigma_w/\bar{u}$ (deg)	σ_u^2 (m^2 sec^{-2})	$\sigma_u^2/\bar{u}^2$
1501–1520										
Corrected statistic	3.42	3.57	4.94	46	2.31	18	0.345	6.8	1.85	0.076
Correction	1.13	1.12	1.12	0	0.80	—	1.37	—	1.28	—
Predicted correction	1.13	1.11	1.13	0	0.81	—	1.34	—	1.30	—
1521–1540										
Corrected statistic	2.88	4.72	5.53	59	3.09	18	0.391	6.5	1.197	0.064
Correction	1.18	1.07	1.10	−2	0.97	—	1.39	—	1.30	—
Predicted correction	1.19	1.06	1.09	−3	0.92	—	1.36	—	1.19	—
1541–1560										
Corrected statistic	1.65	5.28	5.54	73	1.40	12	0.376	6.3	1.65	0.054
Correction	1.31	1.02	1.04	−3	1.19	—	1.38	—	0.99	—
Predicted correction	1.32	1.03	1.05	−4	1.28	—	1.37	—	1.06	—

but the refinement of not making this assumption did not significantly alter the results. This fact and the success of (A4) for correcting the mean winds support the validity of (A11). This assumption was also made by Drinkow (1972) but was neither mentioned nor justified by him.

REFERENCES

Camp, D. W., R. E. Turner and L. P. Gilchrist, 1970: Response tests of cup, vane, and propeller wind sensors. *J. Geophys. Res.*, **75**, 5265–5270.

Clink, W. L., 1971: Comment on "Response tests of cup, vane, and propeller wind sensors." *J. Geophys. Res.*, **76**, 2902.

Drinkow, R.: 1972: A solution to the paired Gill-anemometer response function. *J. Appl. Meteor.*, **11**, 76–80.

Holmes, R. M., G. C. Gill and H. W. Carson, 1964: A propeller-type vertical anemometer. *J. Appl. Meteor.*, **3**, 802–804.

Horst, T. W., 1972: A computer algorithm for correcting non-cosine response in the Gill anemometer. Pacific Northwest Laboratory Annual Report for 1971 to the USAEC Division of Biology and Medicine, Vol. II: Physical Sciences, Part 1: Atmospheric Sciences, BNWL-1651-1. Battelle, Pacific Northwest Laboratories, Richland, Wash. (Available from NTIF, Springfield, Va.).

Kaimal, J. C., 1972: Turbulence spectra, length scales and structure parameters in the stable surface layer. IUCRM Colloquium on Waves and Turbulence in Stable Layers and Their Effects on EM Propagation, San Diego, California.

——, J. C. Wyngaard, Y. Izumi and O. R. Coté, 1972: Spectral characteristics of surface layer turbulence. *Quart. J. Roy. Meteor. Soc.*, **98**, 563–589.

McBean, G. A., 1972: Instrument requirements for eddy correlation measurements. *J. Appl. Meteor.*, **11**, 1078–1084.

MacCready, P. B., Jr., and H. R. Jex, 1964: Response characteristics and meterological utilization of propeller and vane wind sensors. *J. Appl. Meteor.*, **3**, 182–193.